

Characteristic Analysis of Highly-Birefringence Photonic Crystal Fiber Ring Resonator for Resonant Fiber Optic Gyro

Zhenpeng Wang*, Xiaoping Tang, Mingxin Yin, Jinchuan You, and Fei Yu

Abstract—It has attracted the attention of researchers to use photonic crystal fiber (PCF) in the fiber optic gyroscopes (FOG) because of its unique features: radiation insensitivity, high thermal stability, good polarization maintaining ability and low bending loss. In this paper, a PCF-based fiber ring resonator (FRR) as the key sensing component in resonant FOG (RFOG) is experimentally fabricated. The FRR is composed of 10.8 meter long highly birefringent PCF and a traditional polarization maintaining (PM) coupler with PANDA-type pigtail fiber. The resonating characteristics of PCF-based FRR are experimentally tested and as compared with the conventional PM PANDA-type FRR. It is shown that the finesse of PCF-based FRR is about 14. The impacts of structural parameters on the finesse of the PCF-based FRR are also theoretically analyzed. Moreover, the factors that influence the shot-noise limited sensitivity (SLS) of RFOG are numerically discussed. It is of great significance to optimize the structural parameters of FRR and the application of photonic crystal fiber in RFOG.

Index Terms—Photonic crystal fiber; high birefringence; resonant fiber optic gyroscope; limited sensitivity.

I. INTRODUCTION

THE RFOG, also called frequency-sensitive fiber ring gyros, is an type of all-solid-state inertial rotation sensor based on the Sagnac effect [1], [2]. The operating principle of this sensor is that the rotation rate Ω perpendicular to the rotating plane of the FRR is proportional to the resonant frequency difference ΔF between the clockwise and counterclockwise beams of the cavity. In a comparison to the phase-sensitive interferometric fiber optic gyro (IFOG), the frequency-sensitive RFOG has the advantage of a much larger scale factor as the conventional ring laser gyro but avoids the lock-in problem [3]. More importantly, the scale factor of the RFOG does not depend on the length of the fiber coil as does the scale factor of the IFOGs, and the RFOG can achieve the same accuracy by using shorter fiber and has the advantage of small volume [4]. Therefore, it has great potential in high precision and miniaturization in the future, and thus it attracts the interest of a large number of researchers. However, the optical noise in the FRR greatly

limits its accuracy and performance far beyond the theoretical SLS, and slows down its process of the practical application. Polarization fluctuation and backscattering are considered as the main noise sources that deteriorate the performance of RFOG [5], [6]. In order to cope with the aforementioned noises in the RFOG, various suppression methods, such as changing the FRR construction integrating in-line polarizers with twin 90 polarization-axis rotated splices [6] and carrier suppression technique [7], are proposed. However, these countermeasures undoubtedly increase the complexity of the system to a certain extent.

The FRR as the core sensing component plays an important rule in the RFOG, and directly affects or determines the accuracy of the detecting system. PCFs, characterized with air holes arranged along with the fiber length, provides us with a brand new research direction to overcome the optical noise from the root. According to the operating mechanism, the PCF can be divided into two kinds [8], [9]: the total internal reflection PCF (TIR-PCF) and the air-core photonic bandgap fiber (PBF). The PBF guides light to propagate along the fiber in the air medium on account of the photonic bandgap effect, which signifies that it possesses the advantages of better temperature stability, lower Kerr effect and Rayleigh backscattering [10], [11]. However, if the PBF is directly fused connecting with the conventional PM solid-core coupler, the strong Fresnel reflection and great splicing loss will be induced at junctions, which will seriously deteriorate the performance of RFOG [12], [13]. Relatively speaking, the fabrication and welding technology of TIR-PCF is mature at the moment, and is qualified for the RFOG application. Compared with the traditional PM fiber, the TIR-PCF possesses unique characteristics, such as radiation insensitivity, high thermal stability, good polarization maintaining ability, and low bending loss, so it shows great application value in the field of FOGs [14].

In recent years, the PCF-based RFOG has become a hot research topic and attracts the attention of researchers. In References [15], [16], researchers experimentally investigated the temperature dependence of birefringence in the PM TIR-PCF, and verified that the birefringence variation due to temperature change was far smaller than that of the traditional PANDA PMF, which meant that the use of TIR-PCF in RFOG was beneficial to suppress the polarization fluctuations caused by the temperature change. Ying et al [17] theoretically analyzed the sensitivity of the FRR made of an air-core photonic-bandgap fiber (PBF). Yang et al [18] numerically analyzed the temperature effect in the TIR-PCF FRR, and the result also showed that the sensitivity to temperature of TIR-PCF was much lower than that of the

Manuscript received February 7, 2020; revised October 4, 2020. This work was supported in part by the National Natural Science Foundation of China under Grant 51879055, and Grant 51809058.

Z. Wang is with the System Engineering Institute of Sichuan Aerospace, Chengdu, P.R.China (e-mail:wzpdoctor@hrbeu.edu.cn.)

X. Tang is with the System Engineering Institute of Sichuan Aerospace, Chengdu, P.R.China (e-mail: txple1987@126.com)

M. Yin is with the System Engineering Institute of Sichuan Aerospace, Chengdu, P.R.China (e-mail: ymxbuuaa@163.com)

J. You is with the System Engineering Institute of Sichuan Aerospace, Chengdu, P.R.China (e-mail: 103472539@qq.com)

F. Yu is with the Harbin Engineering University, Harbin, P.R.China (e-mail: yufei414@126.com)

conventional fiber. In References [19], [20], the sensitivities of RFOGs, equipped with TIR-PCF, PBF and PANDA fiber, were analyzed and compared in theory, and the simulation results showed that FRRs using the TIR-PCF and PBF had better resonant depth than that of using PMF as well as had nearly the same sensitivity. However, in the above numerical analysis, they only simply considered the influencing factor of transmission-attenuation difference among these types of optical fibers, but ignored some important practical problems like the large splicing loss in the PCF FRR. Wang et al [21] proposed a type of RFOG equipped with the TIR-PCF FRR, and the tested results showed that the finesse of the FRR was only 5.92 but without discussing the cause of the low finesse.

In our previous work, the dynamic characteristics of PCF-based resonators under sinusoidal modulation were theoretically analyzed in detail [22]. This paper experimentally studies the resonating characteristic of the TIR-type PCF FRR, and the comparisons with the PANDA-type FRR are conducted. The impacts of critical structural parameters of PM coupler and fiber on the FRR finesse are also numerically analyzed, which is of great significance to optimize the structural parameters in the FRR. In addition, the dependence of SLS of the RFOG on splicing loss, laser spectral line width, coupling coefficient and total fiber length is theoretically discussed, which is useful for the application of PCF in RFOG.

II. THEORY ANALYSIS

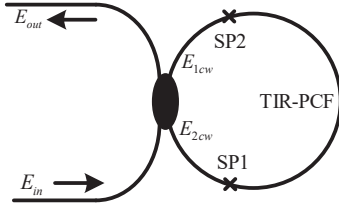


Fig. 1. Simple physical model of a reflective fiber optic resonator

Figure 1 shows the schematic diagram of a PCF FRR consisting of a conventional PM coupler and a length of TIR-PCF. There are two splicing points for fusing the TIR-PCF with the PANDA pigtail fiber of the PM coupler. In the following discussion, the symbols k_c and γ represent the coupler's coupling coefficient and excess loss, and α is the total attenuation coefficients of light transmission around the fiber loop, respectively. The total loss α is composed of two parts: the splicing loss α_s and the fiber transmission attenuation α_L , namely, $\alpha = \alpha_s + \alpha_L$. It is assumed that the total length of the PCF fiber loop is L . According to Figure 1, when the light wave E_{in} is incident into the coupler, a portion of the energy will directly pass through the straight arm of the coupler to the output port. Meanwhile, the rest energy across the coupling arm of the coupler enters into the resonant cavity and propagates along the PCF loop. In each cycle of transmission in FRR, a fraction of energy is coupled out to the output port from the FRR cavity. Finally, the optical interference will happen at the output port.

The input light wave E_{in} can be written as [17]:

$$E_{in} = E_0 \exp j[\omega t + \phi(t)] \quad (1)$$

where E_0 and ω are the amplitude and angular frequency of the light wave, and $\phi(t)$ is the phase fluctuation describing the light source coherence. $\phi(t)$ satisfies:

$$\exp j[\phi(t) - \phi(t - \tau)] = \exp(-2\pi\delta f\tau) = \exp(-\Delta\omega\tau) \quad (2)$$

where δf is the spectral linewidth of the laser, and τ is the time delay. According to the principle of superposition of light waves, the field at the output port can be expressed as:

$$E_{out} = E_0 e^{j\omega t} \left\{ T e^{j\phi(t)} - R' \sum_{n=1}^{\infty} (Q')^{n-1} \cdot \exp j[\phi(t - n\tau) - \omega n\tau] \right\} \quad (3)$$

where

$$\begin{cases} T = \sqrt{1 - k_c} \sqrt{1 - \gamma} \\ R' = k_c(1 - \gamma) \sqrt{1 - \alpha_L} \\ Q' = \sqrt{1 - k_c} \sqrt{1 - \gamma} \sqrt{1 - \alpha_L} \end{cases} \quad (4)$$

$\omega\tau = \beta L$ represents the phase delay of the light transmitting in a circle, and β is the propagation constant of the fundamental mode of the PCF. Substituting Equation (2) into Equation (3), the intensity transfer function of the FRR can be obtained [12], [17]:

$$H = \frac{|E_{out}|^2}{|E_0|^2} = T^2 - \frac{2TR(\cos\omega\tau - Q)}{1 + Q^2 - 2Q\cos\omega\tau} + \frac{(R')^2}{1 - (Q')^2} \frac{1 - Q^2}{1 + Q^2 - 2Q\cos\omega\tau} \quad (5)$$

where

$$\begin{cases} R = k_c(1 - \alpha_c) \sqrt{1 - \alpha_L} e^{\Delta\omega\tau} \\ Q = \sqrt{1 - k_c} \sqrt{1 - \alpha_c} \sqrt{1 - \alpha_L} e^{\Delta\omega\tau} \end{cases} \quad (6)$$

It can be clearly seen that the output intensity of FRR is a function of phase delay $\omega\tau$. According to Equation (5), we can calculate out some characteristic parameters of the resonance curve, and meanwhile the influence of the structural parameters on the resonance curve can be also analyzed. The full width half maximum Γ (FWHM) of the resonance curve is given as [17]:

$$\begin{cases} \Gamma = \frac{1}{\pi\tau} \cos^{-1}(\xi) \\ \xi = \frac{2TRQ[1 - (Q')^2] - 2(R')^2 Q^2}{(TRQ^2 + TR)[1 - (Q')^2] - (R')^2 Q(1 + Q^2)} \end{cases} \quad (7)$$

The SLS is an important parameter to evaluate the performance of the FRR. Shot noise, also known as the photon noise, is a kind of random noise during the process of photoelectric conversion, which determines the minimum detection precision of FOGs. The SLS of RFOG can be theoretically expressed as [23]:

$$\delta\Omega = \frac{n_{eff}\lambda}{D} \frac{\sqrt{2}\Gamma}{SNR} \quad (8)$$

where n_{eff} , λ correspond to the effective refractive index of fundamental mode and the central wavelength of the laser, h and D are Planck's constant and the diameter of the fiber coil, respectively. SNR is the signal-to-noise ratio of the detection system, and can be written as [24]:

$$SNR = \frac{i_s}{i_n} = \sqrt{\frac{\eta t_0 I_0}{2h\nu}} \frac{H_{max} - H_{min}}{\sqrt{H_{max}}} \quad (9)$$

where η is the quantum efficiency of photodetector, t_0 is the integral time, I_0 is the light intensity, ν is the center frequency of the laser, H_{max} and H_{min} are the maximum

and minimum values of the resonant curve, respectively. We can get the values of H_{\max} and H_{\min} by Equation (5):

$$\begin{cases} H_{\min} = T^2 - \frac{2TR}{1-Q} + \frac{(R')^2}{1-(Q')^2} \frac{1+Q}{1-Q} \\ H_{\max} = T^2 + \frac{2TR}{1+Q} + \frac{(R')^2}{1-(Q')^2} \frac{1-Q}{1+Q} \end{cases} \quad (10)$$

Then, the SLS formula can be further expressed as:

$$\delta\Omega = \frac{n_{eff}\lambda}{D} \sqrt{\frac{hv}{\eta t_0 I_0} \frac{2\Gamma\sqrt{H_{\max}}}{H_{\max} - H_{\min}}} \quad (11)$$

Obviously, when the incident light intensity is fixed, the SLS of RFOG mainly depends on the values H_{\max} and H_{\min} , namely the resonance characteristics of FRR. The resonance characteristics and finesse of FRR are related to the structural parameters of PM coupler and fiber, so it is necessary to optimize parameters of FRR to achieve the high performance. Actually, the total transmission loss α , especially the splicing loss at the splicing points of PCF FRR is much larger than that of traditional PANDA-type fiber, which will lead to some difference for resonance characteristics between PCF-based FRR and PANDA-type FRR.

III. SIMULATION AND EXPERIMENT

A. Resonance Characteristics Analysis

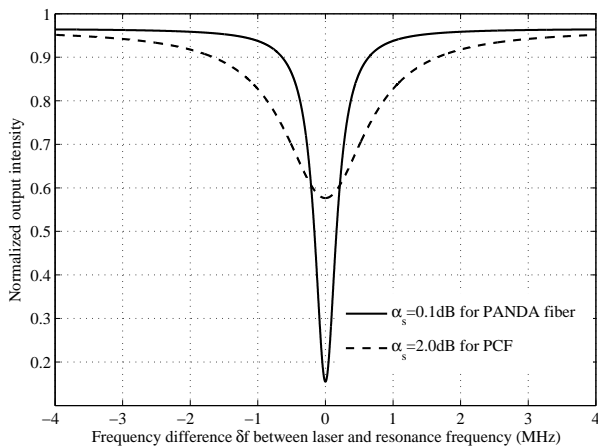


Fig. 2. Theoretical resonance curves for the different splicing loss α_s corresponding to the PANDA-type FRR and PCF FRR.

We firstly numerically analyze the influence of the splicing loss α_s on the resonance curve of FRR. In the simulation, the parameters are set as $\delta f = 30$ kHz, $\lambda = 1.55 \mu\text{m}$, $L = 10.8$ m, $D = 10$ cm, $n = 1.44$, $k_c = 5\%$, and $\gamma = 0.15$ dB. Meanwhile, the fiber transmission attenuation α_L is reasonably ignored, namely, $\alpha \approx \alpha_s$, because it is as low as 0.005 dB and 0.02 dB for 10 meter long PANDA-type fiber and TIR-PCF, far less than the splicing loss α_s . Figure 2 shows the simulated resonance curves with $\alpha_s = 0.1$ and 2.0 dB corresponding to the PANDA-type FRR and PCF-type FRR, respectively. It can be clearly seen that the PCF resonant curve (red dashed line) has a smaller resonance depth and larger FWHM, which results in a lower resonance finesse.

Then, two types of FRRs with PM PANDA-type fiber and PM TIR-PCF are experimentally fabricated. Here, two identical traditional PM fiber couplers with $k_c = 5\%$ and

$\gamma = 0.15$ dB are employed, and the mode field diameter of the coupler's PANDA-type pigtail fiber in the fast and slow axis are almost the same about $6.5 \mu\text{m}$ at the wavelength of $1.55 \mu\text{m}$. It is well known that the PANDA-type FRR can be easily fabricated with low splicing loss about 0.05 dB. The PCF-based FRR consists of a traditional PM coupler and a length of 10.8 m PM TIR-PCF that contains two enlarged air holes in the cross section to produce high birefringence like that in References [15], [16]. For the geometric parameters of the used PM PCF, the hole pitch Λ , the diameters of the small air holes d and the two large air holes D are $4.4 \mu\text{m}$, $2.2 \mu\text{m}$ and $5 \mu\text{m}$, respectively. The PCF's mode field diameters are about $6.2/3.2 \mu\text{m}$ at $\lambda = 1.55 \mu\text{m}$. Since the mode field of the used PM PCF is elliptical shape, it doesn't perfectly matched with the circular mode field of PANDA fiber, which will bring about large fusing splicing loss at the splicing point [25]. Theoretically speaking, the fusion loss caused by the field mismatch is more than 1 dB for one splicing point. Fortunately, the mode field of PCF is able to be optionally tuned by controlling the collapse of air holes using traditional arc fusion splicer [26], [27]. In the fusion process, we carefully adjust the fusion time or fusion current to change the PCF's mode field for the purpose of the mode-field matching. After repeated attempts, the splicing loss of a single fusion point for the PCF can be reduced to be about 0.65 dB, and thus the total splicing loss α_s in the PCF FRR is about 1.3 dB. The photo of the fabricated PCF-based FRR can be seen in Figure 3, where a PIN-FET photodetector with the PANDA-type pigtail fiber is applied.

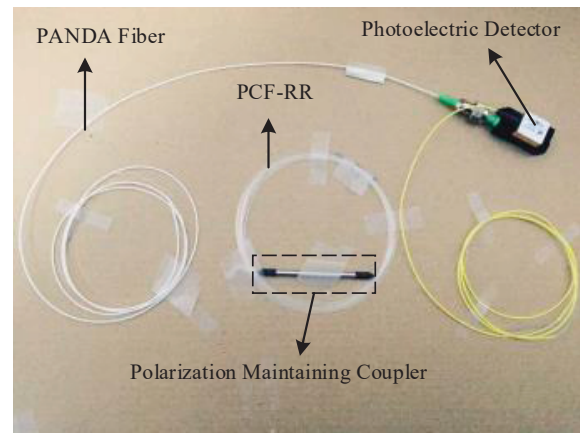


Fig. 3. The fabricated PCF-based resonator with a traditional PM coupler.

To test the resonant curve of FRRs, the experiment platform is set up. In the test system, the light emitted from narrowlinewidth laser, $\delta f \leq 0.1$ kHz, firstly passes through an optical isolator to avoid reflected power worsening the performance of the light source. At the output port of the cavity, a photoelectric detector is connected to an oscilloscope and the resonance curve can be displayed when we adjust the laser's output central frequency through the computer terminal. It should be noted that all components in the system are PM devices with the extinction ratio greater than 25 dB. Figure 4(a) and 4(b) show the experimental resonance curves of the PANDA FRR and the PCF-based FRR, respectively. We can see that the resonance curve of the PANDA FRR is much sharper than that of the PCF FRR, and the finesse of the two types of cavities are 14 and 72. The finesse of the PCF FRR

fabricated by us is two times higher than that in Reference [21]. Meanwhile, it has to be recognized that the finesse of PCF-based FRR is still smaller than that of PANDA-type FRR due to the large splicing loss between the PCF and the PM coupler even though the mode field matching technique is further optimized.

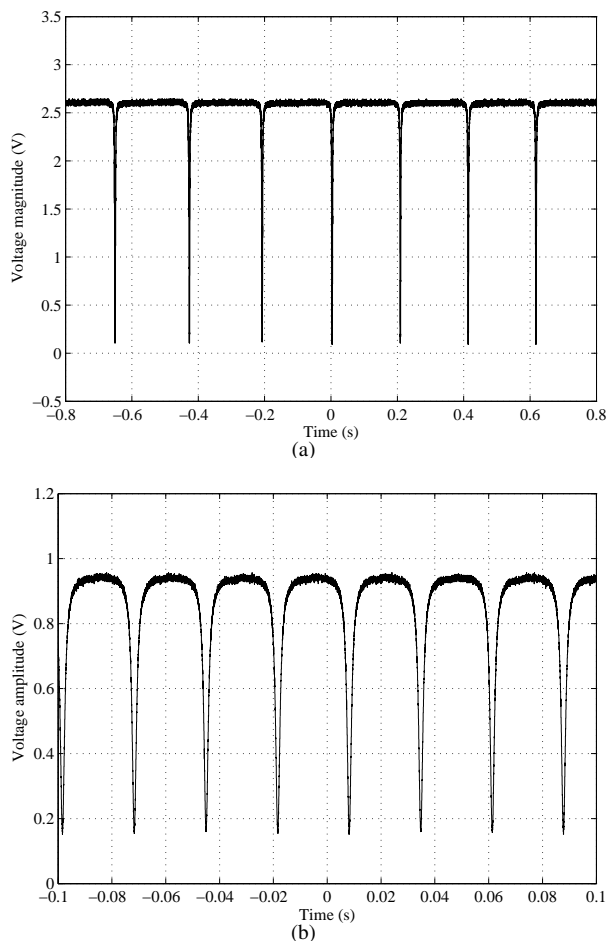


Fig. 4. Experimental resonance curves of (a) the PANDA-type FRR (b) the PCF-based FRR

B. Shot-noise Limited Sensitivity Analysis

As the core sensing component in the RFOG, the FRR directly influences or determines the RFOG's detecting precision. To achieve high detecting sensitivity, it is necessary to optimize structural parameters and investigate their influence on the sensitivity. The structural parameters are the splicing loss α_s , the linewidth δf of laser, the coupling coefficient k_c and excess loss γ of the coupler, and the total length L of FRR.

1) *Impact of splicing loss and laser linewidth:* To analyze the impact of α_s on the RFOG performance, the dependent relationship between SLS and the splicing loss α_s is numerically studied, as shown in Figure 5. The simulation parameters are assumed to be as follows: the intensity I_0 of the incident light is 1 mW, the integral time t_0 is 1 s, the responsivity of photoelectric detector is 0.85 A/mW, and the other parameters are the same as mentioned above. Figure 5 shows that with the increase of α_s the value of SLS apparently becomes larger corresponding to a lower sensitivity for RFOG. When the splicing loss increases from

0 to 3 dB, the SLS of RFOG varies from $0.02^\circ/h$ to $0.9^\circ/h$. Particularly, if we want the sensitivity to be higher than $0.1^\circ/h$, the loss α_s should be controlled below 0.6 dB. It is a great challenge for the TIR-PCF to achieve such low loss for two splicing points in the PCF FRR under the current fiber-fusion technology.

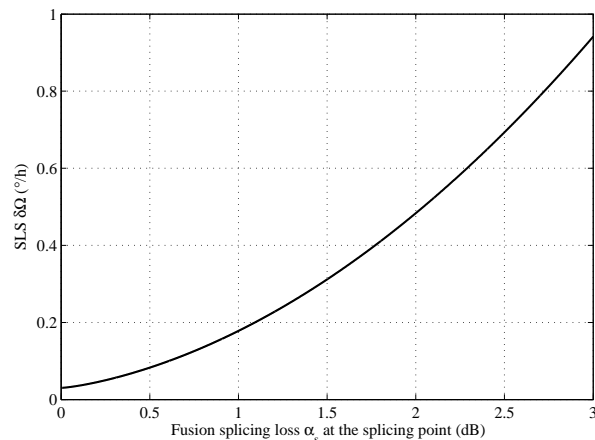


Fig. 5. The dependent relationship between the RFOG SLS and the splicing loss α_s .

The impact of the laser spectral linewidth on SLS is also studied as illustrated in Figure 6, where it is clear that increasing the laser linewidth will deteriorate the RFOG sensitivity. Therefore, the RFOG detecting system usually employs a extremely narrow-linewidth laser (typically $\delta f \leq 100\text{kHz}$) so as to make the sensitivity as high as possible. In addition, the RFOG SLS of the PCF FRR is less sensitive than that of the PANDA FRR under the same laser linewidth, the reason of which is because the finesse of PCF-based FRR is smaller than that of PANDA FRR.

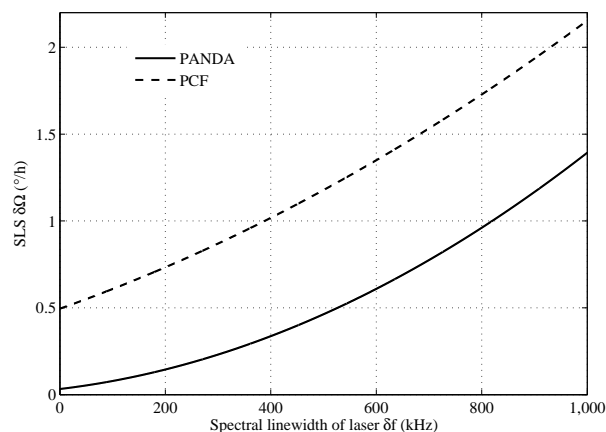


Fig. 6. The impact of the laser spectral linewidth on the RFOG SLS for the PANDA FRR and PCF FRR.

2) *Impact of coupler structural parameters:* The PM coupler is the most important part of FRR, and it should have a high extinction ratio as far as possible for the polarization stability. When we fabricate the fiber resonator, the first problem is how to confirm the coupler's structural parameters: the coupling coefficient k_c and the excess loss γ . Figure 7 illuminates the dependent relationship between the RFOG SLS and the coupling coefficient k_c for the two types of FRRs. It can be observed that there is an

optimal coupling coefficient $k_c = k_c^p$ that makes RFOG most sensitive. The optimal value k_c is 2% for the PANDA-type FRR corresponding to the best SLS of $0.04^\circ/h$ while for the PCF FRR the most appropriate k_c is about 20% with the best RFOG SLS of $0.25^\circ/h$. It can be also seen that with k_c increasing from the optimal value, the SLS for the PANDA FRR becomes worse while that for the PCF FRR almost keeps unchanged. In other words, the RFOG SLS with higher finesse FRR is more sensitive to the change of coupling coefficient k_c . From the point of view of the RFOG SLS, the PM coupler for the PCF-base FRR can be chosen in a larger range with k_c varying from 10% to 40%.

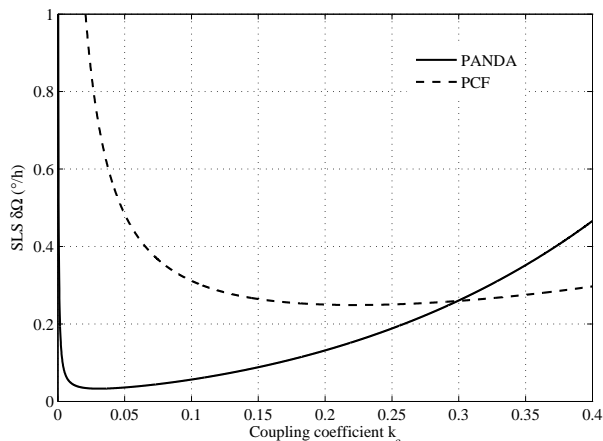


Fig. 7. The dependent relationship between SLS and the coupling coefficient k_c of the PM coupler.

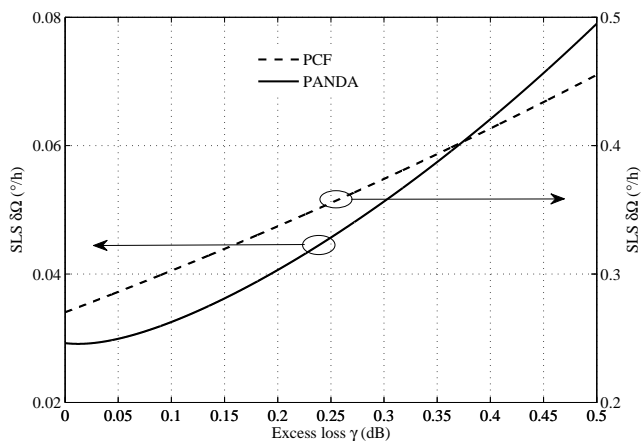


Fig. 8. The impact of the coupler's excess loss γ on SLS for the PANDA FRR and PCF FRR.

The excess loss γ of PM coupler is defined as the power reduction of all output ports with respect to the input power, which reflects the inherent loss in the device manufacturing process. Figure 8 shows the dependent relationship between the coupler excess loss γ and SLS for the PANDA FRR and PCF FRR. It can be clearly observed that the value of the sensitivity becomes larger with the increase of γ for both fiber resonators. Therefore, the smaller the excess loss γ is, the more sensitive the RFOG detecting system is. The excess loss γ is normally around 0.2 dB that corresponds to the theoretical RFOG sensitivities of $0.04^\circ/h$ and $0.35^\circ/h$ for the two types of FRRs. It should be noted that for the above experiments in Section III-A, we specially customize

the commercial PM coupler with a excess loss of 0.15 dB to improve the detecting sensitivity as much as possible.

3) *Impact of total fiber length:* According to the formula $\Delta F = D \cdot \Omega / n_{eff} \lambda$, it seems that the detection accuracy of RFOG is only related to the diameter of the FRR and independent of the length of the fiber. However, the fiber length L of FRR does indeed impacts the RFOG sensitivity [3]. Figure 9 shows the impact of the total fiber length L on the RFOG SLS for the PANDA-type FRR and PCF FRR. The unit attenuation coefficient of the PANDA fiber and TIR-PCF are respectively assumed to be 0.5 dB/km and 2 dB/km with $k_c = 5\%$ in the simulation. We can find that the blue and red curves in Figure 9 have the same change tendency in which the sensitivity increases initially and then reduces as the fiber length L increases. The sensitivity using the PANDA-type FRR reaches the peak of $0.02^\circ/h$ when the fiber length L is 50 m. However, for the PCF FRR the fiber length L corresponding to the highest sensitivity is about 200 m which is almost four times longer than that of the PANDA-type FRR. Finally, it is clear that the sensitivity of RFOG has little variation when the fiber length exceeds 100 m, and thus the fiber length of FRR can be chosen to be about tens of meters, not more than 100 meters.

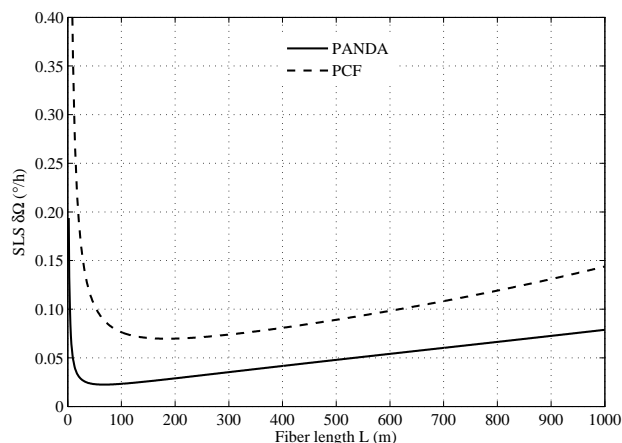


Fig. 9. The impact of the total fiber length L on the RFOG SLS for the PANDA-type FRR and PCF FRR.

IV. CONCLUSION AND DISCUSSION

In this research, two types of FRRs, highly birefringent PCF FRR and PANDA-type FRR, are experimentally fabricated. The tested resonant curve indicates that the finesse of the PCF FRR fabricated by us is about 14 that is more than two times higher than that in Reference [9], which profits from the optimized fiber fusion technique. Thereafter, the dependent relationships between the RFOG SLS and structural parameters are theoretically analyzed and compared for both FRRs. From the simulated results, we can draw the following conclusions: 1) The splicing loss α_s is a very critical factor to influence the RFOG detecting performance especially for the PCF FRR. The lower the splicing loss α_s in the FRR, the higher the sensitivity of the RFOG detecting system; 2) The smaller spectral line-width δf of laser in RFOG system can lead to the higher RFOG sensitivity. The laser with line-width δf less than 10 kHz is recommended to achieve a high sensitivity; 3) The RFOG sensitivity will get deteriorative with the increase of the excess loss γ of the coupler. The

excess loss γ should be less than 0.2 dB when we choose the PM fiber coupler; 4) There is an optimal coupling coefficient k_c making the RFOG SLS most sensitive, and the RFOG SLS with higher finesse FRR is more sensitive to the variation of coupling coefficient k_c ; 6) Too long fiber length not only cannot increase the sensitivity of RFOG, but will make it worse on the contrary. It is enough for the fiber length of FRR being tens of meters. The above theoretical analysis is of guiding significance to the optimization of FRR structural parameters.

From the above experimental and theoretical analysis, it has to be recognized that the finesse of PCF FRR is still smaller than that of PANDA-based FRR because of the large splicing loss between PCF and PANDA-type fiber. However, the PCF resonator has inherent benefits for reducing the optical noises in the RFOG, and the application of PCF in the RFOG has great potential in improving its performance when all aspects of the factors are considered. It is believed that the problem of large fusion splicing loss for PCFs is expected to be resolved with the improvement of the fiber fusion technology in the future.

REFERENCES

- [1] S. Ezekiel and S. R. Balsamo, "Passive ring resonator laser gyroscope," *Applied Physics Letters*, vol. 30, no. 9, pp478-481, 1977.
- [2] G. A. Sanders, M. G. Prentiss, and S. Ezekiel, "Passive ring resonator method for sensitive inertial rotation measurements in geophysics and relativity," *Optics Letters*, vol. 6, no. 11, pp569-571, 1981.
- [3] W. W. Chow, J. Gea-Banacloche, L. M. Pedrotti, V. E. Sanders, W. Schleich, and M. O. Scully, "The ring laser gyro," *Reviews of Modern Physics*, vol. 57, no. 1, pp61-104, 1985.
- [4] L. Wang, Y. Yan, H. Ma, and Z. Jin, "Resonant fiber optic gyro based on a sinusoidal wave modulation and square wave demodulation technique," *Applied Optics*, vol. 55, no. 12, pp3274-3278, 2016.
- [5] X. Yu, H. Ma, and Z. Jin, "Improving thermal stability of a resonator fiber optic gyro employing a polarizing resonator," *Optics Express*, vol. 21, no. 1, pp358-369, 2013.
- [6] H. Ma, X. Yu, and Z. Jin, "Reduction of polarization-fluctuation induced drift in resonator fiber optic gyro by a resonator-integrating in-line polarizers," *Optics Letters*, vol. 37, no. 16, pp3342-3344, 2012.
- [7] H. Ma, X. Chang, Z. Yang, and Z. Jin, "Full investigation of the backscattering in resonator fiber optic gyro," *Optics Communications*, vol. 284, no. 19, pp4480-4484, 2011.
- [8] T. P. Hansen, J. Broeng, S. E. B. Libori, E. Knudsen, and H. Simonsen, "Highly birefringent index-guiding photonic crystal fibers," *IEEE Photonics Technology Letters*, vol. 13, no. 6, pp588-590, 2001.
- [9] X. L. Zhang, W. Jin, and D. Q. Ying, "Performance analysis of an optical passive ring-resonator gyro with a hollow-core photonic bandgap fiber sensing coil," in *Proceedings of SPIE, Advanced Sensor Systems and Applications*, vol. 7853, pp785324, 2010.
- [10] Md. Omar Faruk, Md. Belayat Hossain, and Md. Shafiul Islam, "Effect of lattice constant and air hole diameter on the mode profile in triangular and square lattice photonic crystal fiber at THZ regime," in *Proceedings of World Congress on Engineering and Computer Science*, 2010.
- [11] C. C. Liao, "Design of high birefringence and low-loss index-guiding photonic crystal fiber by modified elliptical air holes in fiber cladding," in *Proceedings of the International MultiConference of Engineers*, pp1669-1672, 2012.
- [12] L. Feng, X. Ren, X. Deng, and H. Liu, "Analysis of a hollow core photonic bandgap fiber ring resonator based on micro-optical structure," *Optics Express*, vol. 20, no. 16, pp18202-18208, 2012.
- [13] Y. Yan, H. Ma, L. Wang, H. Li, and Z. Jin, "Effect of Fresnel reflections in a hybrid air-core photonic-bandgap fiber ring-resonator gyro," *Optics Express*, vol. 23, no. 24, pp31384-31392, 2015.
- [14] Jesse Tawney, Farhad Hakimi, R. L. Willig, John Alonzo, and Dennis J. Trevor, "Photonic crystal fiber IFOGs," in *Proceedings of Optical Fiber Sensors*, 2006.
- [15] P. Ma, N. Song, J. Jin, J. Song, and X. Xu, "Birefringence sensitivity to temperature of polarization maintaining photonic crystal fibers," *Optics & Laser Technology*, vol. 44, no. 6, pp1829-1833, 2012.
- [16] H. Zhao, M. Chen, and G. Li, "Temperature dependence of birefringence in polarization-maintaining photonic crystal fibres," *Chinese Physics B*, vol. 21, no. 6, pp068404, 2012.
- [17] D. Ying, M. S. Demokan, X. Zhang, and W. Jin, "Sensitivity analysis of a fiber ring resonator based on an air-core photonic-bandgap fiber," *Optical Fiber Technology*, vol. 16, no. 4, pp217-221, 2010.
- [18] W. Wang, and B. Yang, "Analysis of temperature effect in fiber optics ring resonator based on photonic crystal fiber," *Optik*, vol. 126, no. 19, pp2094-2098, 2015.
- [19] B. Yang, L. Sun, Y. Li, and M. Fu, "Characteristics analysis of fiber optic ring resonator based on photonic crystal fiber," *Optik*, vol. 130, pp287-290, 2017.
- [20] X. Li, Z. Xu, Y. Hong, P. Liu and W. Ling, "Comparative analysis of fiber ring resonator based on different fibers," *Optik*, vol. 127, no. 5, pp2954-2958, 2016.
- [21] L. Wang, H. Li, H. Ma, and Z. Jin, "Resonant fiber optic gyro based on total internal reflection photonic crystal fiber ring resonator," in *Conference of Asia Pacific Optical Sensors*, 2016.
- [22] Z. Wang, G. Wang, W. Gao, Z. Wang, Z. Wang, and W. Miao, "Resonator optimization of the resonant fiber optic gyro under dynamic condition," in *Proceedings of Position, Location and Navigation Symposium*, pp31-33, 2018.
- [23] R. E. Meyer, S. Ezekiel, D. W. Stowe, and V. J. Tekippe, "Passive fiber-optic ring resonator for rotation sensing," *Optics Letters*, vol. 8, no. 12, pp644-646, 1983.
- [24] D. M. Shupe, "Fiber resonator gyroscope: sensitivity and thermal nonreciprocity," *Applied Optics*, vol. 20, no. 2, pp286-289, 1981.
- [25] H. Li, Y. Yang, and W. Yang, "Mode field measurement and discharge-redress techniques for polarization maintaining photonic crystal fibers," *Acta Optica Sinica*, vol. 35, no. 2, pp0206001, 2015.
- [26] L. Xiao, W. Jin, and M. S. Demokan, "Low-loss splicing small-core photonic crystal fibers and single-mode fibers by repeated arc discharges," in *Conference on Lasers and Electro-Optics*, 2007.
- [27] X. Zhou, Z. Chen, H. Chen, and J. Hou, "Fusion splicing small-core photonic crystal fibers and single-mode fibers by controlled air hole collapse," *Optics Communications*, vol. 285, no. 24, pp5283-5286, 2012.

Zhenpeng Wang received the M.S. and Ph.D. degrees from the College of Automation, Harbin Engineering University, Harbin, China, in 2013 and 2017, respectively. He is currently an engineer of the Sichuan Academy of Aerospace Technology. His research interests include fiber optic gyro, photonic crystal fiber, inertial navigation systems, and aircraft attitude control.

Xiaoping Tang received his B.S. and M.S. degrees in engineering from Harbin Engineering University, Harbin, China, in 2010 and 2013, respectively. His current research interests include flight vehicle design.

Mingxin Yin received his B.S. degree in Aircraft Design Engineering from Beijing University of Aeronautics and Astronautics, Beijing, China, in 2012, and the M.S. degree in GNC from The Third Academy of China Astronautics, Beijing, China, in 2015. His current research interests include aircraft design, formation control, flight control, and guidance law design.

Jinchuan You received the Ph.D. degrees from the College of Automation, Northwestern Polytechnic University, Xi'AN, China, in 2014. He is currently an engineer of the Sichuan Academy of Aerospace Technology. His research interests include inertial navigation systems, and initial alignment, integrated navigation.

Fei Yu received the B.S. degree from the Dalian University of Technology, Dalian, China, in 1997, and the M.E. and Ph.D. degrees from Harbin Engineering University, Harbin, China, in 2003 and 2005, respectively, where he is currently a Professor with Science College. His research interests include ship strapdown inertial navigation technology and integrated navigation technology.